Covalent bonding and hole–electron Coulomb interaction U in C_{60} on Be(0001) surfaces

2007 J. Phys.: Condens. Matter 19 176009

(http://iopscience.iop.org/0953-8984/19/17/176009)

IOP PUBLISHING JOURNAL OF PHYSICS: CONDENSED MATTER

J. Phys.: Condens. Matter **19** (2007) 176009 (15pp) doi:10.1088/0953-8984/19/17/176009

Covalent bonding and hole–electron Coulomb interaction U in C_{60} on Be(0001) surfaces

C T Tzeng[1,2], K D Tsuei[1,3,5], H M Cheng[3,4] and R Y Chu[3,4]

[1] National Synchrotron Radiation Research Centre, Hsinchu 30076, Taiwan, Republic of China
[2] Department of Electronic Engineering, Lan-Yang Institute of Technology, I-Lan 261, Taiwan, Republic of China
[3] Department of Physics, National Tsing Hua University, Hsinchu 30013, Taiwan, Republic of China
[4] Industrial Technology Research Institute, Hsinchu 310, Taiwan, Republic of China

E-mail: tsuei@nsrrc.org.tw

Received 23 January 2007, in final form 28 March 2007
Published 16 April 2007
Online at stacks.iop.org/JPhysCM/19/176009

Abstract

We have investigated the bonding nature and hole–electron Coulomb interaction U in thin C_{60} films on Be(0001) surfaces using valence-band and core-level photoemission, inverse photoemission, and near-edge x-ray absorption spectroscopies. The C_{60} monolayer had strong covalent bonding with the Be substrate, producing a nearly insulating film, in contrast to a metallic overlayer due to charge transfer observed on many other metallic surfaces. The effect of polarization of surrounding molecules and the image potential decreases the energy gap and U, but the bonding–antibonding contribution increases the gap at the interface. The measured U in thin solid films agrees well with a model calculation using gas-phase values. The deduced hole–electron attraction on the surface is about 0.7 eV larger than the reported hole–hole repulsion determined by Auger spectroscopy. On the basis of the surface–solid difference, the newly estimated value of U for hole–hole correlation places doped C_{60} compounds nearer the metallic side of a Mott transition.

1. Introduction

The interface of C_{60} with surfaces has attracted much interest [1–35]. It stems from the rich physical and chemical properties in pure solids and bulk compounds [1], and is viewed as a prototypical molecular device in research on molecular electronics [2]. Through its large ionization energy and small electron affinity, a C_{60} molecule is an ineffective electron donor but an effective electron acceptor. As a result, alkali doping can transfer electrons to C_{60} solid to form stable compounds (A_xC_{60}, A = alkali). In particular, compounds with

[5] Author to whom any correspondence should be addressed.

0953-8984/07/176009+15$30.00

half-filled LUMO ($x = 3$) are metallic and become superconducting at low temperatures. The most direct evidence of charge transfer is the observation of filled LUMO near the Fermi energy in photoemission [3]. Charge transfer that is expected to occur on metallic surfaces has been observed for a monolayer (ML) C_{60} on all polycrystalline noble-metal surfaces [4, 5] and crystalline Au(110), [6, 7] Au(111) [8–10], Cu(110) [11], Cu(111) [12–14], Ag(110) [15, 16], Ag(111) [17–19], and Ag(100) [20]. This effect has been categorized as a signature of ionic bonding [21], but on electron-rich Al(111) and Al(110) substrates that also have a small work function, no charge transfer was observed in photoemission and the bonding was identified as covalent [21]. It is more difficult to observe charge transfer in photoemission on transition-metal surfaces because of their large d-band density of states at the Fermi level. Covalent bonding has been observed for a ML C_{60} on Ni(110) [22, 23], Pt(111) [22, 23], Rh(111) [24], Ta(110) [25, 26], and Mo(110) [27]. In those systems C_{60} even decomposes at elevated temperatures due to the strong bonding. C_{60} was found to decompose also on noble-metal surfaces with a large charge transfer observed, such as Ag(100) [20] and Cu(111) [28], although C_{60} is reported to desorb on Cu(111) [29]. Decomposition of C_{60} was not invariably observed on transition-metal surfaces such as W(100) [30] and Ni(111) [28]. No charge-transfer state was observed in C_{60} on semiconductor surfaces such as Si(111) [31, 32], Si(100) [33], and Ge(111) [34, 35]. In such cases no new (charge-transfer) feature is observed at the Fermi energy, and the HOMO and HOMO $-$ 1 are considerably broadened; this condition is strong evidence of covalent bonding [21]. There are other characteristic features associated with covalent bonding, such as a narrow C 1s core-level peak in photoemission, with its satellite structures nearly washed out, and the upward shift of the LUMO in C 1s x-ray absorption spectra [21, 36]. The bonding of C_{60} to surfaces is classifiable as these types: weak predominantly van der Waals, intermediate predominantly covalent, strong predominantly covalent, intermediate predominantly ionic [21], and strong predominantly ionic [20]. One measure of the strength of a substrate–adsorbate bond is the temperature of desorption or decomposition [21].

The magnitude of the molecular C_{60} on-site Coulomb interaction U has played a significant role in understanding the bulk superconductivity of A_3C_{60} [37–40]. If the ratio U/W, with W ($\sim$0.5 eV) the band width, is larger than a critical value ($\sim$2.5 in [40]) the compound is a Mott–Hubbard insulator, while if the ratio is smaller than the critical value the compound can be described as a correlated metal. U in terms of hole–hole repulsion has been experimentally measured from Auger spectra to be 1.6 ± 0.2 eV [37] or 1.4 ± 0.2 eV [39] in thick C_{60} films. This condition puts A_3C_{60} near the borderline; it has been argued theoretically that A_3C_{60} is on the metallic side of a Mott–Hubbard transition [40]. The reduced energy gap and U of C_{60} in the proximity of a Ag(111) surface has been discussed in terms of image-potential screening and the extent of reduction could be understood semi-quantitatively [41]. Experimentally, $U = 0.6$ eV, which is much smaller than in bulk C_{60}.

We have measured photoemission (PES), inverse photoemission (IPES) and C 1s near-edge x-ray absorption spectra (XAS) of the system C_{60} on a Be(0001) surface, which exhibits properties of C_{60} on both metal and semiconductor surfaces. Image-potential screening on metal surfaces is strong and observed in this case. A nearly insulating overlayer and strong covalent bonding are also observed, and these properties are similar to systems of C_{60} on many semiconductor surfaces, because of the characteristics of Be metal. Be has a small density of states at the Fermi energy and can be viewed as a semi-metal. There is a large band gap around the zone centre [42, 43] of the Be(0001) surface, and charge transfer from the substrate to the LUMO found in noble-metal systems would be minimized. For a 3 ML film the measured energy gap and U agree well with a result of a model calculation adapted from [41], using gas-phase values and including solid-state effects. The deduced energy gap and U for a surface

are larger than previously reported values on thick films also using photoemission and inverse photoemission spectroscopies [41]; and the deduced U is about 0.7 eV larger than measured from Auger spectra [37, 39]. On the basis of the surface–solid difference, the estimated value of U for hole–hole correlation energy places doped C_{60} compounds near the metallic side of a Mott transition. For 1 ML C_{60}/Be the observed energy gap tends to be increased by covalent bonding, in a direction opposite to the decrease from image-potential screening. The carbon 1s core correlation energy U_c is only slightly smaller than the valence band U.

2. Experiments

The experiments were performed at the National Synchrotron Radiation Research Centre (NSRRC) in Hsinchu, Taiwan using beam line HSGM and at the IPES lab in NTHU. The photoemission and near-edge XAS were measured in an ultrahigh-vacuum chamber equipped with low-energy electron diffraction (LEED) and a hemispherical analyser (radius 200 mm) aligned at a fixed angle 50° to the incident photon beam. The base pressure was less than 1×10^{-10} Torr. For valence-band photoemission, a UV lamp provided photons of energy 21.22 eV (He I) and the angular acceptance was ±1°. For C 1s core-level photoemission an acceptance angle ±8° and photon energy 320 eV were used. The overall energy resolution was 0.15 eV for valence-band and 0.4 eV for core-level measurements. We determined the work function by measuring the photoemission at the secondary edge rise and the Fermi level cut-off, with a sample bias −10 eV. Using the known photon energy (He I) and subtracting the total spectrum width yields the absolute work function. For the C 1s near-edge XAS measurement, we used total electron yield detection and normalized the signal to the photocurrent from a freshly evaporated Au mesh placed before the sample. The photon energy was calibrated with photoemission from second-order light. The IPES was measured in a separate ultrahigh-vacuum chamber equipped with LEED, a grating spectrograph, and a 2D detector system; the base pressure was less than 1×10^{-10} Torr. The angular acceptance was ±4°; the incident beam was normal to the surface. The incident electron energy was 20.24 eV; the overall energy resolution was 0.5 eV.

The crystal was cleaned with cycles of sputtering with 1.5 keV Ar ions and annealing until a sharp LEED pattern was observed. A cleaning procedure was established to ensure that no measurable C and O contamination was observed from core-level photoemission [44]. The C_{60} was evaporated from a resistively heated Ta evaporator. The pressure rise during deposition was less than 2×10^{-10} Torr. The deposition and measurements were done at room temperature (RT). A small rate of growth (5–20 min per layer) served to favour growth layer by layer. As the desorption temperature of multilayer C_{60} (∼180 °C) [17] is near the decomposition temperature of C_{60} on Be (between 200 and 250 °C) [44], the commonly used method to produce an ordered monolayer by annealing was inapplicable. No overlayer LEED pattern was observed, indicating a lack of long-range order. This condition is partly due to a large mismatch between the C_{60} and Be lattice parameters. The attenuation of the clean Be(0001) surface state was used to calibrate the monolayer dosage. In addition, the binding energy of the C 1s core level shifted when the second layer began to grow; this calibration yielded the same rate of evaporation.

3. Results and discussion

3.1. Valence-band photoemission and inverse photoemission

The normal emission valence-band photoemission spectra for clean Be(0001), 1 ML C_{60}/Be (0001) and 3 ML C_{60} are displayed in figure 1. For a clean surface the primary peak at a

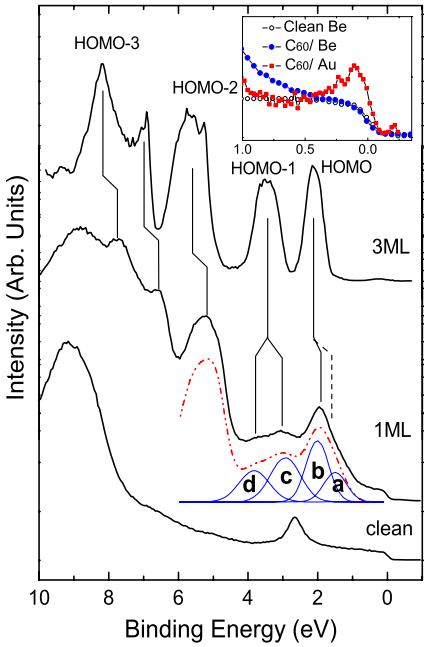

Figure 1. Photoemission spectra for clean Be(0001), 1 ML (unannealed) and 3 ML C_{60} on Be surfaces. The observed peak shifts are labelled with solid lines while the expected rigid shift of HOMO is labelled with a dashed line. A curve fit to the 1 ML spectrum after removing the background is shown below. The spectra are normalized to the sample current. The inset compares the spectra of 1 ML and a clean surface near the Fermi level after removing the He I satellite contribution. The spectrum of C_{60}/Au(111) measured at 22 eV extracted from [10] is included to show the charge-transfer feature.

(This figure is in colour only in the electronic version)

binding energy 2.7 eV is a surface state on Be(0001); another feature about 9 eV binding energy is a bulk transition in the Be substrate [42]. For the 3 ML film the HOMO, HOMO − 1, and HOMO − 2 are at 2.1, 3.5 and 5.7 eV, respectively, and the HOMO − 3 features are at 8.2 and 6.95 eV [45]. The weak feature near the Fermi level in the 3 ML spectrum was the HOMO peak excited by the 1.9 eV higher-energy satellite of the He I source. For the 1 ML spectrum the HOMO and HOMO − 1 features were considerably broadened relative to those for 3 ML. This broadening arises from the interaction between C_{60} and the substrate with site and possibly orientation variation. There appeared two features near the expected energy of the HOMO − 1. One might attribute one of these two features to the shifted Be surface state, but the intensity of either decomposed component shown in figure 1 seems much higher than that of the surface state of the clean surface, making a direct linkage unlikely. These two features might arise from the energy splitting of h_g and g_g states, which are degenerate for an isolated molecule [46], but the splitting is more likely due to bonding and non-bonding with substrate states as is discussed later. The broadening and splitting of the HOMO and HOMO − 1 reflect hybridization interaction between C_{60} and the Be(0001) surface.

Figure 2 shows IPES spectra for C_{60} on Be(0001) at various coverages. The signals associated with C_{60} molecular orbitals become more intense with increasing thickness. For the 2.2 ML spectrum the three low-lying features at 1.58, 2.8 and 3.75 eV above the Fermi level are identified as LUMO, LUMO + 1, and LUMO + 2, respectively. We see that the

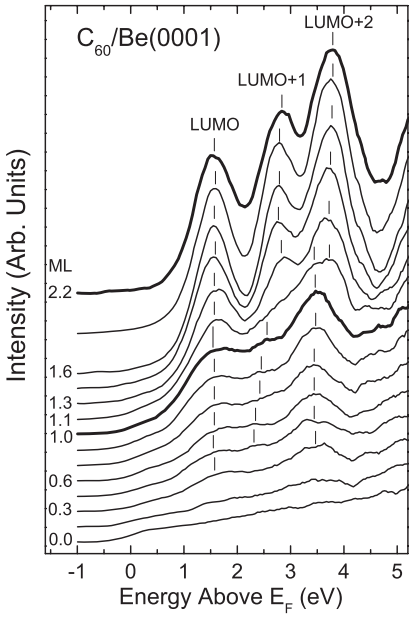

Figure 2. Inverse photoemission spectra for clean Be(0001), and C_{60} coverages up to 2.2 ML on Be surfaces. The incident electron energy was 20.24 eV. The spectra are normalized to sample current. For the submonolayer spectra the statistics might be less good; the ticks mark the approximate position of the feature.

Table 1. Measured binding energies of HOMOs and LUMOs in eV.

	HOMO − 3	HOMO − 2	HOMO − 1	HOMO	LUMO	LUMO + 1	LUMO + 2
3 ML	8.2, 6.95	5.7	3.5	2.1	1.6[a]	2.8[a]	3.75[a]
1 ML	7.75, 6.5	5.25	3.7, 3.0	1.93	1.6	2.5	3.5
3 − 1 ML[b]	0.45	0.45	−0.2, 0.5	0.17	0.0	0.3	0.25

[a] The estimated difference 0.02 eV between 3 ML and 2.2 ML is added to this value.
[b] The positive values indicate an upward shift for HOMOs and a downward shift for LUMOs.

features in the sub-monolayer spectra are much less pronounced than those in the 2.2 ML spectrum, presumably due to large broadening caused by site and possibly orientation variation and interaction with the substrate. For sub-monolayer coverage the LUMO and LUMO + 2 remain at about constant energies 1.6 and 3.5 eV, respectively, while the LUMO + 1 feature was weak but discernible even as small as 0.4 ML, as marked approximately by ticks. Some shift might be observable. At 1 ML or less, the LUMO + 1 was not observed in IPES of C_{60} on Cu(111) [14] and Au(110) [47] at RT, but was on Ag(111) [41]. As the coverage increased above 1 ML the LUMO position remained almost unchanged while LUMO + 2 shifted toward 3.75 eV. The LUMO + 1 feature became more prominent and sharper as the other two peaks. As we discuss later, all three low-lying states have an interaction with the Be substrate, as in C_{60}/Au(110) [47]. We summarize in table 1 the energies of the peaks and their shifts observed in both photoemission and inverse photoemission.

The low intensity at the Fermi level in the clean Be(0001) surface spectrum in both photoemission and inverse photoemission spectra collected in normal geometry reflected the bulk projected band gap at the Γ-point from 4.2 eV below the Fermi level up to 1.2 eV

above [42, 43]. The finite intensity was due to scattering from residual roughness, which is expected not to depend on the light polarization. The Be surface state is sp_z derived, and can be excited only with p-polarized light at normal emission. Because we used unpolarized light, the relative intensity at the Fermi level to the surface state is enhanced relative to spectra measured using p-polarized synchrotron radiation [42]. The inset of figure 1 compares the spectra of 1 ML and a clean surface near the Fermi energy after removal of the He I satellite contribution. No new feature appeared just below the Fermi energy, in contrast to systems of C_{60} on noble-metal surfaces for which a charge-transfer feature from the substrate to LUMO was observed, [10, 13, 19, 20, 28] for example C_{60}/Au(111), as also shown in the inset. Spectra collected at off-normal emission geometry (not shown) showed no state crossing the Fermi energy either. Figures 1 and 2 show that there was no intensity change evident at the Fermi energy within 1 ML coverage relative to spectra for the clean surface in both photoemission and inverse photoemission, and no obvious contribution to the Fermi energy intensity from either the HOMO or the LUMO was identified[6]. These observations indicate that charge transfer did not occur from the Be substrate to the LUMO. In addition the HOMO and HOMO − 1 are considerably broadened or split. According to [21] for C_{60}/Al, these situations are strong evidence for covalent bonding. According to further evidence that we will present, these observations are also consistent with the C_{60} ML remaining insulating, or nearly insulating. This nearly insulating property of the C_{60} ML is closely related to the semi-metallic property of the Be substrate, unlike most other metal substrates that have generally a much larger density of states at the Fermi energy. Moreover, this insulating property is similar to that observed for C_{60} on semiconductor surfaces [31–35].

Close examination of the peak energies reveals that the three major features of HOMO − 2 and HOMO − 3 in the 1 ML photoemission spectrum shift upward uniformly by 0.45 eV relative to the 3 ML spectrum. These low-lying molecular orbitals are derived primarily from both σ and π states; in contrast the high-lying HOMO and HOMO − 1 have contributions from only π states. The σ orbitals residing within the cage surface are less perturbed by, or have weaker interaction with, the substrate than the protruding π orbitals. Both energy and orbital considerations strongly indicate that the uniform shift of HOMO − 2 and HOMO − 3 results from a common origin, which is not due to chemical bonding.

Before discussing a quantitative analysis, we note that, for the kinetic energies of electrons that we used to probe the sample, the mean free path is less than the typical interlayer spacing [49]. As a result the photoemission and inverse photoemission data were dominated by signals from the outermost molecular layer of C_{60}. This small mean free path is consistent with our core-level photoemission data at similar kinetic energies. Thus we assume that the signals were from only the outermost molecular layer in the subsequent analysis, following [41].

The most likely reason for a uniform shift in our photoemission data is the final-state screening of the hole left behind in the photoemission process. One kind of screening is from the polarization of neighbouring molecules, as has been applied successfully to the bulk and surface of C_{60} films [37, 38, 50]. The polarization energy is expressed as $E_p = 0.5z\alpha e^2/R^4$, in which α is the C_{60} molecular polarizability ($\alpha = 90$ Å) [51][7], z is the coordination number ($z = 6$ for ML, 9 for surface, and 12 for bulk for an fcc(111) surface, according to [41]), and R is the inter-molecular distance (10.02 Å). The calculated value is 0.065 eV per neighbour. It has also been identified in C_{60}/Ag(111) that in the proximity of a metal surface the image-potential screening to the final-state hole or electron is expressible for 1 ML as $E_{ip} = 0.5e^2/2d$,

[6] For 1 ML C_{60}/Be the residual intensity at the Fermi energy might arise from the metal substrate scattered by surface roughness of the substrate with attenuation and the additional scattering through the incommensurate C_{60} overlayer lacking long-range order.

[7] The dielectric constant ε was measured to be 4.4, from which α can be deduced using the Clausius–Mossotti relation.

in which d is the distance from the centre of the probed molecule to the image plane [41]. The total relaxation energy is the sum of the polarization energy and image potential energy and is responsible for the final-state screening difference between 3 ML and 1 ML in photoemission. The value d becomes an adjustable parameter to fit the experimentally observed difference. Using the best value $d = 5.3$ Å for the first ML the calculated image-potential screening is 0.68 eV. For 3 ML the distance from the topmost layer to the image plane should be used in the evaluation of the image potential energy, which becomes further decreased by the dielectric screening of the C_{60} layer in between, i.e., divided by the dielectric constant $\varepsilon = 4.4$, from [51]. This latter approximation yields a contribution only 0.04 eV to the image-potential screening for 3 ML, indicating that the detail of the approximation is unimportant. The total relaxation energy is thus 0.62 eV for 3 ML and 1.07 eV for 1 ML, with a difference 0.45 eV the same as the observed upward shift in photoemission. Similarly, the screening of the electron final state in inverse photoemission is expected to result in a downward shift.

The experimentally determined distance 5.3 Å between the centre of the first ML and the image plane is slightly larger than half the distance between C_{60} molecules, and it places the image plane between the first ML C_{60} and the surface layer of Be. This value is reasonable because for most metal surfaces the image planes are located near the jellium edge or half the interplanar distance beyond the surface layer [52]. This assignment is again consistent with the first ML being nearly insulating [13, 14].

Once the 0.45 eV shift has been attributed to final-state screening of weakly interacting or non-bonding molecular orbitals, we discuss the relative shift of high-lying HOMO and LUMO. We expect that the same extent of final-state shift would occur in PES and IPES of these high-lying orbitals. The HOMO signal for 1 ML, shifted upward only 0.17 eV, had actually a downward shift $0.45 - 0.17 = 0.28$ eV, and in contrast the LUMO signal had an upward shift $0.45 - 0.0 = 0.45$ eV. These initial-state shifts reflect the bonding–antibonding (B–AB) energy shifts of the first ML C_{60} interacting with the Be surface. An apparent 0.4 eV upward shift of the C 1s to a LUMO resonance for ML relative to a spectrum of the thick film was also observed in XAS as is discussed later. This covalent bonding nature differs markedly from C_{60} adsorbed on noble-metal surfaces for which a metallic C_{60} ML due to a substrate charge transfer was observed [4–20]. Covalent bonding is consistent with no charge transfer and the first ML remains nearly insulating. From the apparent shift as listed in table 1, we deduce that the LUMO + 1 and LUMO + 2 orbitals for 1 ML have upward antibonding shifts $0.45 - 0.3 = 0.15$ and $0.45 - 0.25 = 0.2$ eV, respectively.

For 1 ML C_{60}/Al(110) a splitting of HOMO into two components was clearly observed while HOMO − 1 showed a broad feature [2]. A fitting procedure was applied to separate HOMO − 1 also into two components. These two HOMO features were interpreted as due to symmetry selecting two HOMO orbitals with the lower binding-energy feature being due to the orbital with a strong overlap with the substrate and the higher binding-energy signal being due to the orbital with little overlap with the substrate, i.e., a different orientation of degenerate orbitals. The energy separation is due mainly to different final-state screening. In our case of 1 ML C_{60}/Be, the HOMO − 1 was split into two components while the HOMO shows a single feature but much broader than that of the thicker film. We performed a curve fit to separate both HOMO − 1 and HOMO into two components each, as shown below the 1 ML spectrum in figure 1. A background similar to the clean surface spectrum without the surface state was subtracted. A Gaussian line shape is used for all four features with both the HOMO − 1 and HOMO pairs having the same individual widths. As the line shape is unknown, the peak positions from the fit are only approximate. This satisfactory fit indicates that the HOMO also likely splits into two components. Both the lower binding-energy components of HOMO and HOMO − 1, peaks a and c, respectively, have their energy shift relative to the 3 ML film

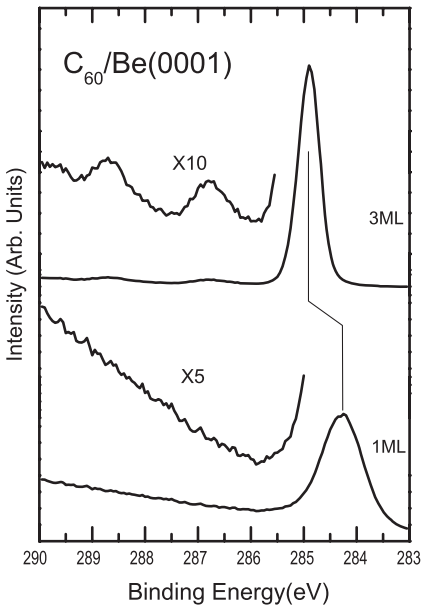

Figure 3. C 1s core-level photoemission spectra for a 3 ML and an unannealed 1 ML film. The intensity in the satellite region has been multiplied by the factors shown at left.

near 0.45 eV. This condition lends support to assigning the lower binding-energy components to non-bonding orbitals with the substrate, and the higher binding-energy components to bonding orbitals with the substrate. Both components have the same final-state shift, but different initial-state energies.

The splitting of the HOMO into two peaks has been observed also for C_{60} on several semiconductor surfaces, including Si(111) [31, 32], Si(100) [33], and Ge(111) [34, 35]. No charge transfer was observed in these systems, and the interaction was concluded to be covalent bonding. The higher binding-energy peak of the HOMO was interpreted as the bonding state between the C_{60} carbon atoms and the substrate atoms [34]; the lower binding-energy peak was the shifted HOMO [32], and the spectra are similar for overlayers with and without long-range order [34]. This assignment of the split HOMO is consistent with our interpretation. Be is a semi-metal for which the surface state of Be(0001) renders this surface metallic. Upon chemisorption of C_{60} the surface state becomes removed. The small density of states at the Fermi energy can still provide metallic image-potential screening.

3.2. Core-level photoemission

Figure 3 shows the carbon 1s core level and satellite region of 1 ML and 3 ML C_{60} on the Be(0001) surface. For the 1 ML spectrum the line is broadened relative to the 3 ML film, reflecting an interaction with the substrate. The line shape is nearly symmetric although still narrow compared to other systems. These features resemble those of covalently bound systems such as C_{60}/Al(110), C_{60}/Al(111) [21] and C_{60}/Pt(111) [23, 36, 48]. The satellite features for thick films are shake-up and plasmon excitations [7, 13]. The broadening of the shake-up structures in the ML films can be regarded as a measure of the bonding interaction with the substrate, and for covalently bound systems these structures are nearly totally washed

out [23, 53]. The small relative energy region is sometimes obscured by the asymmetric tail of the main line especially in charge-transferred systems [7, 10, 13, 21, 27, 48, 53]. These satellite features in this region are observed completely lacking from the 1 ML C_{60}/Be spectrum because of a narrow and nearly symmetric main line. Hence the covalent bonding in C_{60}/Be is stronger than that in C_{60}/Al in which the first few satellite features remain [21], but nearer C_{60}/Pt(111) [48, 53]. We emphasize that the decomposition temperature of C_{60} on Be surfaces between 200 and 250 °C is the least among the systems studied so far [44], consistent with strong covalent bonding [21].

The C 1s core-level binding energy of 1 ML C_{60}/Be(0001) shifts to the lower binding-energy side with a value 0.6 eV relative to the 3 ML film. This value is larger than the expected rigid shift 0.45 eV from the valence band. A crude estimate on the basis of a pure image-potential effect to explain the extra 0.15 eV shift would place the effective core hole position 1 Å below the centre of the molecule—a large and unrealistic value, as is discussed below. One might estimate also the effect of the image potential by assuming the core hole to be located at individual atoms. With 0.5 eV broadening to simulate the observed width, we obtained an asymmetric line shape with a tail extending towards the low binding-energy side [10, 13]. The apparent line position would have a binding energy greater than that calculated at the centre, contrary to the experimental observation. Although a core electron is localized at individual atoms, from a measurement of core-level photoemission and a calculation the core hole was concluded to be effectively screened by valence states within the ionized molecule, so that the core hole appears from the outside to be centred on the C_{60} cage [50]. This effect served to explain the rigid shift of the C 1s core level with the σ-like levels in C_{60}/Al [21]. These considerations indicate that pure image-potential screening cannot explain the experimental observation. We tentatively attribute the 0.15 eV difference to the C 1s core-level (initial-state) chemical shift.

3.3. XAS near C K edge

The carbon K-edge XAS spectra for 1 ML C_{60}/Be and a thick film are displayed in figure 4. The XAS spectra are essentially invariant above 2 ML, consistent with previous work [13]. For the thick-film spectrum, the first peak at 284.5 eV marks a C 1s transition to the π^* LUMO. The next three lines at 285.8, 286.4 and 288.3 eV might be labelled LUMO + 1, LUMO + 2 and LUMO + 3 respectively, and represent excitation to the π^* orbitals [7, 13]. For the ML spectrum the LUMO + 1 line in XAS failed to appear because of interaction with the substrate, similar to many other systems [7, 10, 21], but it appeared in C_{60}/Au(111) [13]. In contrast LUMO + 1 was present in IPES, reflecting different final states coupled to the substrates in these two techniques. All peaks were considerably broadened for the 1 ML C_{60}/Be XAS spectrum. The C 1s to LUMO resonance shifts 0.4 eV upward relative to the spectrum of the thick film. The LUMO + 2 and LUMO + 3 resonances have upward shifts 0.1 and 0.2 eV, respectively. A similar upward shift of the LUMO had been observed for C_{60}/Al [21], and was believed to be due to covalent bonding (antibonding), while LUMO + 2 and LUMO + 3 shift downward in those systems. In C_{60}/Be the extent of upward shift of LUMO is larger, indicating strong covalent bonding, consistent with the previous conclusion based on the suppression of the satellite region of the C 1s core level. No final (charge) state effect would occur in a neutral excitation in XAS; thus the observed upward shift due to antibonding is not obscured such as by the downward shift from the negative-charge final state in IPES. The energies of peaks observed in core-level photoemission and XAS are summarized in table 2.

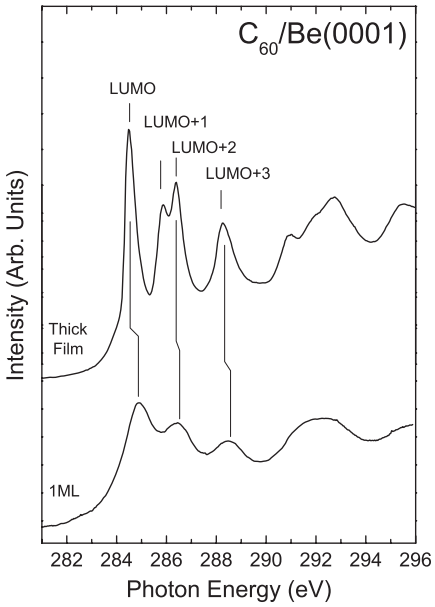

Figure 4. C 1s near-edge XAS for 1 ML (unannealed) and thick films.

Table 2. Measured C 1s binding energies and XAS energies in eV.

	C 1s[a]	C 1s → LUMO	C 1s → LUMO + 1	C 1s → LUMO + 2	C 1s → LUMO + 3
3 ML	284.9	284.5	285.8	286.4	288.3
1 ML	284.3	284.9		286.5	288.5
3 ML − 1 ML[b]	0.6	0.4		0.1	0.2

[a] Core-level binding energy.
[b] The positive value for C 1s core level and XAS are for an upward shift in energy.

In a metallic system such as C_{60}/Cu(111) [13] the C 1s binding energy coincides with the absorption threshold, and marks the Fermi-edge position in XAS [53]. For the covalently bound C_{60}/Al systems there are also clear features near the onset of absorption, which coincide with the C 1s binding energy [21]. In contrast the system C_{60}/Be behaves quite differently. The position corresponding to the C 1s binding energy is nearer the LUMO peak, while it is about 2 eV above the apparent threshold, nearer the case of a thick film that is insulating. Hence the metallic screening strength in XAS of C_{60}/Be is much weaker than both the metallic C_{60}/Cu(111) and covalent C_{60}/Al. This presents a clear evidence that the C_{60} ML on a Be surface cannot be metallic, consistent with the inference from photoemission and inverse photoemission that the C_{60} ML is nearly insulating.

The LUMO feature is broadened but not attenuated in our spectra. The LUMO is thus not filled with electrons transferred from the substrate, consistent with the photoemission and inverse photoemission observations. Combining all spectroscopic results and the fact that C_{60} decomposes at a low temperature on Be surfaces, we conclude that the interaction between C_{60} and the Be substrate is strong covalent bonding with no charge transfer, in the same category as on the Ni(110), Pt(111), and the Si and Ge surfaces, according to the classification of bonding types in [21].

3.4. Work function

The measured work function of 1 ML C_{60} on Be(0001) was 5.0 ± 0.1 eV, which is 0.15 eV less than that of a clean surface. In many charge-transferred C_{60}/metal systems the work-function change cannot be simply explained by placing an image plane between the C_{60} monolayer and the substrate surface layer and calculating the dipole formation due to transferred charge [10, 13, 21]. In C_{60}/Be a work function decrease was observed despite no charge transfer. This effect is likely due to charge redistribution on covalent bonding, forming net dipoles across the interface [54]. An *ab initio* calculation on C_{60}/Cu(111) reveals multipolar charge redistribution at the interface [55]. Experimental investigations of organic molecules on metal surfaces demonstrated that the repulsion between electrons on the molecule and on the metal surface produces a compression of the electron tail spilling out from the metal surface into the vacuum causing a decreased metal work function [56, 57]. A work function near 5 eV is commonly observed in many 1 ML C_{60}/metal systems [10, 13, 21]. The measured work function of a 2 ML film was identical to that of the 1 ML film, reflecting the weak (van der Waals) interaction between the two layers. If we further assume the work function for 3 ML approximately the same as that of the 2 ML film [58] we find that the measured HOMO position in photoemission relative to the vacuum level would become $5.0 + 2.1 = 7.1 \pm 0.1$ eV, in reasonable agreement with the reported ionization energy (6.90 ± 0.04 eV) for solid C_{60} films [58], and also with the estimated ionization energy from a surface molecule from the gas-phase value [59] including the solid polarization and substrate image-potential screening effects as discussed previously ($7.58 - 0.065 \times 9 - 0.04 = 6.955$ eV). Hence the C_{60} MOs align with the vacuum level for the 3 ML film [58].

3.5. Coulomb correlation energy U

The definition of Hubbard correlation energy U in C_{60} is generally given as $U = E_I - E_A - \Delta$, in which E_I is the ionization energy, E_A is the electron affinity, and Δ is the excitation energy on site from the HOMO to the LUMO [37]. With this definition U is the energy difference between the locally excited molecule and removing the excited electron to a remote site, or the exciton binding energy, and can thus be viewed as a valence hole–electron Coulomb interaction (attraction).

The magnitude of U in C_{60} solids was estimated also from gas-phase values considering the polarization of surrounding molecules [37], but the result was larger than the measured values. It has been argued that in close proximity of a Ag(111) surface the energy gap and U of the first ML C_{60} would be further reduced by image-potential screening and the magnitude of reduction of the energy gap and U can be understood semi-quantitatively including both effects [41].

We can extract U from our photoemission and inverse photoemission results. The substrate Fermi level provides a common reference for both techniques, replacing the vacuum level. The sum of HOMO binding energy in photoemission and LUMO energy in inverse photoemission, or the energy gap, is equal to $\Delta + U$. From the measured gap 3.7 eV with an excitation energy 1.6 eV for a solid film measured by high-resolution electron energy-loss spectroscopy (HREELS) [24, 60] it is straightforward to deduce U from the above equation to be 2.1 eV for 3 ML.

For comparison we calculate the energy gap and U using gas-phase values of ionization energy 7.58 eV [59], electron affinity 2.69 eV [61], and HOMO–LUMO excitation energy 1.57 eV [61], including solid-state and substrate–metallic screening effects in the model mentioned previously. For the 3 ML and 1 ML films the experimentally determined

Table 3. Measured and calculated HOMO–LUMO energy gap and U of C_{60} for the valence-band exciton binding energy and measured core exciton binding energy U_c in eV.

	Measured gap	Measured U	Calculated gap	Calculated U
3 ML	3.7	2.1[a]	3.65	2.08
1 ML	3.53/3.25[b]		2.75	1.18
Gas phase			4.89	3.32
Surface			3.73	2.16
Solid			3.33	1.76
3 ML (U_c)		2.0		
1 ML (U_c)		1.0		

[a] An excitation energy 1.6 eV from [24] and [60] is used to extract U for 3 ML.
[b] For measured HOMO B–LUMO AB and approximate HOMO NB–LUMO AB gaps.

image-plane distance is used. Both the measured and calculated energy gaps and U are compared in table 3. The calculated values of energy gap 3.65 eV and U 2.08 eV for 3 ML are in *excellent agreement* with the measured values. *Not only the reduction of these values* [41] *but also their absolute values are quantitatively reproduced*. This fact enables us confidently to calculate U on surfaces and in solids using the same model.

The calculated U for C_{60} solid surfaces and in solids is then 2.2 and 1.8 eV, respectively (see table 3), with an estimated uncertainty less than 0.1 eV. The average valence (HOMOs) hole–hole Coulomb repulsion has been measured previously as 1.6 ± 0.2 eV (1.4 eV for HOMO) [37] and 1.4 ± 0.2 eV [39] on comparing Auger electron spectra with self-convolution of the valence photoemission spectra. As most Auger electrons come from the outermost surface layer, its value should be compared with our surface value; the discrepancy about 0.7 eV is substantial. This discrepancy is attributed to the fact that the (HOMO) hole and the (LUMO) electron tend to stay close together while the two holes (in HOMOs) tend to stay apart; thus the hole–electron attraction energy is larger than the hole–hole repulsion energy, according to [40] and [62]. Similarly using photoemission and inverse photoemission data, U has been determined to be 1.7 eV for the surface of a thick film [41], much smaller than our value 2.2 eV using thin films. The source of the discrepancy is unclear. We note that for thick films charging effects were observed in IPES [37], which tends to increase the apparent energy and for which a manual correction was needed, resulting in some uncertainty in the measured energy gap. The use of a 3 ML thin film can totally remove such a charging effect and avoid a correction. We note that for 3 ML the measured U, 2.1 eV, serves as the lower limit of the surface U, irrespective of the model for calculating U on a surface. Thicker films can lead only to energies away from the metal–substrate Fermi level and a larger U.

As the hole–hole Coulomb repulsion might be more representative of the two-electron correlation in the LUMO in alkali-doped C_{60}, one can estimate the correlation energy in solids from the surface-sensitive Auger values, 1.6 eV in [37] or 1.4 eV in [39], by subtracting the surface–solid difference 0.4 eV from our model calculation [41]. The deduced U is about 1.0–1.2 eV in a solid, near the calculated U values 1.27 eV [63] or 0.8–1.3 eV [62]. The ratio U/W becomes about 2.2, slightly less than the border line at 2.5, indicating that doped C_{60} is nearer a correlated metal than a Mott insulator [40]. Experimentally, A_3C_{60} are metals while A_1C_{60} and A_4C_{60} are insulators, indicating a variation of critical values of U/W, or other intricate balance factors, across the Mott transition.

For the ML the extraction of U is more complicated. For the HOMO both bonding (B) and non-bonding (NB) components were observed while only the antibonding (AB) state of the LUMO was observed in C_{60}/Be. The deduced values of the HOMO–LUMO energy gap are

then 3.53 and 3.25 eV, for B–AB, and NB–AB pairs, respectively. Comparing to the calculated value 2.75 eV for a ML assuming no interaction with the substrate, it is clear that the energy gap can become increased by the covalent bonding–antibonding effect. For this non-interacting ML the excitation energy Δ is expected to be similar to that of a gas-phase molecule (1.57 eV) or in a solid (1.6 eV), and the calculated U becomes 1.18 eV using the former value. Because bonding–antibonding is an initial-state effect with no charge change, and because the HOMO–LUMO excitation Δ involves only neutral states, we argue that it is reasonable to assume B–AB to increase Δ by a similar amount. The resulting U would be about 1.2 eV for both HOMO–LUMO pairs, near that of a non-interacting insulating ML. This cancellation effect of the B–AB shift was observed in the core exciton binding energy U_c, as is discussed later.

For charge-transferred systems or metallic C_{60} ML the situation can differ. For 1 ML C_{60}/Ag(111)Δ was deduced to be 1.6 eV, almost the same as the gas-phase and solid values, from the PES by doping the ML film with K until the LUMO is completely filled [41]. Δ is thus claimed to be insensitive to the chemical environment and to the charge state of the molecule [36]. Hence U for C_{60}/Ag(111) is determined to be 0.6 eV [41]. Similarly for C_{60}/Au(110), which is also metallic [48], U is deduced to be 0.5 eV using 1.6 eV as Δ [36]. These values of U are substantially smaller than that of a non-interacting insulating ML, or the covalently bound nearly insulating C_{60}/Be, as we have argued. If we apply the same model to both metallic cases, the resulting image-plane position would be 3.8 and 3.6 Å to the centre of C_{60} ML, for C_{60}/Ag and C_{60}/Au, respectively. These values are near the radius of a C_{60} molecule, 3.5 Å measured to the nuclei, and are near the maximum of the MO wavefunction [45]. In these cases the simple image-potential form for a hole in HOMO or an electron in LOMO would fail. Moreover, the polarization energy comes from the dipole moment induced at nearby molecules by an electric field generated from the final-state hole or electron. For metallic C_{60} ML that has partially filled LUMO bands [13], the screening within the metallic ML can attenuate the electric field and the polarization energy, rendering the simple form invalid. We conclude that the simple model of polarization and image-potential screening is questionable in the case of charge-transferred metallic C_{60} ML. For the nearly insulating C_{60} ML on Be the image plane is well outside the molecules, and the model is expected to remain applicable.

The C 1s core exciton binding energy U_c can be determined in a similar fashion from the measured C 1s core-level binding energy, plus the LUMO energy in IPES, minus the C 1s to LUMO excitation energy from XAS. For 3 ML the deduced U_c, 2.0 eV, is near the valence–exciton binding energy U, 2.1 eV. This similarity indicates that in both the core excitation processes to LUMO in XAS and to states well above the ionization threshold as in PES the core hole becomes effectively screened by the valence states such that it behaves like a valence (HOMO) hole. For 1 ML the deduced U_c, 1.0 eV, is also near the calculated valence U, 1.2 eV, of a ML not interacting with the substrate. This similarity indicates that the effect of the covalent antibonding that causes a shift of the LUMO in IPES produces a similar shift in XAS; these shifts almost cancel in the calculation of U_c. This cancellation effect would also occur in the valence U for 1 ML, supporting our previous argument of U being about 1.2 eV. These values are compared in table 3. For thick films a value $U_c = 2.2 \pm 0.3$ eV has been reported [38] on combining an experimentally determined C 1s ionization energy and gas-phase values in a model similar to the one used here, in close agreement with our results.

4. Conclusions

We have investigated C_{60} on a Be(0001) surface by photoemission, inverse photoemission, and near-edge XAS spectroscopies. The splitting of the HOMO $-$ 1 and HOMO peaks and the total

suppression of C 1s core-level photoemission satellite spectra for ML C_{60} on Be(0001) indicate a strong interaction between the C_{60} molecule and the Be substrate. There is no evidence of charge transfer in PES, IPES and XAS. The C_{60} overlayer on Be(0001) surface is therefore nearly insulating. In addition, the bonding and antibonding effect of the C_{60} molecular orbitals interacting with the Be(0001) substrate are identified. Along with the fact that C_{60} decomposes at a low temperature on Be surfaces the interaction between C_{60} molecules and the Be(0001) surface is thus concluded to be strong covalent bonding.

The valence hole–electron Coulomb attraction (Hubbard U) and core hole–electron Coulomb attraction (U_c) for C_{60} films on the Be substrate are extracted from the combination of PES, IPES and XAS. The Hubbard U for 3 ML C_{60} on the Be substrate is determined to be 2.1 eV, in excellent agreement with a model calculation using gas-phase values and simple solid-state effects, including polarization of neighbouring molecules and metal–substrate image-potential screening. The solid-surface difference can be used to correct U of the hole–hole repulsion measured from Auger and photoemission spectra to be near results of more advanced calculations, and to place the alkali-doped C_{60} closer to a correlated metal than a Mott insulator.

We demonstrate for the first time that the covalent bonding effect for the C_{60} ML on metal surfaces tends to increase the energy gap, in the direction opposite from the decrease due to image-potential screening by the metal surface; and is important in charge transport across the molecule–metal electrode interface in modern molecular electronic devices.

Acknowledgments

The National Synchrotron Radiation Research Centre and the National Science Council of the ROC supported this work. KDT thanks E W Plummer for supplying the Be sample and H T Jeng and C S Hsue for providing their molecular-orbital calculation and many stimulating discussions.

References

[1] Dresselhaus M S, Dresselhaus G and Eklund P C 1996 *Science of Fullerenes and Carbon Nanotubes* (San Diego, CA: Academic)
[2] Schiessling J, Stener M, Balasubramanian T, Kjeldgaard L, Decleva P, Norgren J and Brühwiler P A 2004 *J. Phys.: Condens. Matter* **16** L407
[3] Benning P J, Poirier D M, Ohno T R, Chen Y, Jost M B, Stepniak F, Kroll G H, Weaver J H, Fure J and Smalley R E 1992 *Phys. Rev.* B **45** 6899
[4] Chase S J, Bacsa W S, Mitch M G, Pilione L J and Lannin J S 1992 *Phys. Rev.* B **46** 7873
[5] Hoogenboom B W, Hesper R, Tjeng L H and Sawatzky G A 1998 *Phys. Rev.* B **57** 11939
[6] Modesti S, Cerasari S and Rudolf P 1993 *Phys. Rev. Lett.* **71** 2469
[7] Maxwell A J, Brühwiler P A, Nilsson A, Mårtensson N and Rudolf P 1994 *Phys. Rev.* B **49** 10717
[8] Altman E I and Colton R J 1993 *Surf. Sci.* **295** 13
[9] Altman E I and Colton R J 1993 *Phys. Rev.* B **48** 18244
[10] Tzeng C T, Lo W S, Yuh J Y, Chu R Y and Tsuei K D 2000 *Phys. Rev.* B **61** 2263
[11] Murray P W, Pedersen M Ø, Lægsgaard E, Stensgaard I and Besenbacher F 1997 *Phys. Rev.* B **55** 9360
[12] Hashizume T and Sakurai T 1994 *J. Vac. Sci. Technol.* B **12** 1992
[13] Tsuei K D, Yuh J Y, Tzeng C T, Chu R Y, Chung S C and Tsang K L 1997 *Phys. Rev.* B **56** 15412
[14] Tsuei K D and Johnson P D 1997 *Solid State Commun.* **101** 337
[15] Purdie D, Bernhoff H and Reihl B 1996 *Surf. Sci.* **364** 279
[16] Magnano E, Vandré S, Cepek C, Goldoni A, Laine A D, Curro G M, Santaniello A and Sancrotti M 1997 *Surf. Sci.* **377–379** 1066
[17] Tjeng L H, Hesper R, Heessels A C L, Heeres A, Jonkmann H T and Sawatzky G A 1997 *Solid State Commun.* **103** 31

[18] Wertheim G K and Buchanan D N E 1994 *Phys. Rev.* B **50** 11070
[19] Yang W L, Brouet V, Zhou X J, Choi H J, Louie S G, Cohen M L, Kellar S A, Bogdanov P V, Lanzara A, Goldoni A, Parmigiani F, Hussain Z and Shen Z-X 2003 *Science* **300** 303
[20] Goldoni A and Paolucci G 1999 *Surf. Sci.* **437** 353
[21] Maxwell A J, Brühwiler P A, Arvanitis D, Hasselstrom J, Johansson M K J and Mårtensson N 1998 *Phys. Rev.* B **57** 7312
[22] Cepek C, Goldoni A and Modesti S 1996 *Phys. Rev.* B **53** 7466
[23] Pedio M, Hevesi K, Zema N, Capozi M, Perfetti P, Gottebaron R, Pireaux J J, Caudano R and Rudolf P 1999 *Surf. Sci.* **437** 249
[24] Sellidj A and Koel B E 1993 *J. Phys. Chem.* **97** 10076
Jiang L Q and Koel B E 1994 *Phys. Rev. Lett.* **72** 140
[25] Ruckman M W, Xia B and Qiu S L 1993 *Phys. Rev.* B **48** 15457
[26] Rudolf P and Gensterblum G 1994 *Phys. Rev.* B **50** 12215
[27] Hunt M R C, Rajogopal A, Caudano R and Rudolf P 2000 *Surf. Sci.* **454–456** 267
[28] Tzeng C T and Tsuei K D, unpublished
[29] Silien C, Marenne I, Auerhammer J, Tagmatarchis N, Prassides K, Thiry P A and Rudolf P 2001 *Surf. Sci.* **482–485** 1
[30] Wertheim G K and Buchanan D N E 1993 *Solid State Commun.* **88** 97
[31] Cepek C, Schiavuta P, Sancrotti M and Pedio M 1999 *Phys. Rev.* B **60** 2068
[32] Sakamoto K, Harada M, Kondo D, Kimura A, Kakizaki A and Suto S 1998 *Phys. Rev.* B **58** 13951
[33] Seta M D, Sanvitto D and Evangelisti F 1999 *Phys. Rev.* B **59** 9878
[34] Goldoni A, Cepek C, Seta M D, Avila J, Asensio M C and Sancrotti M 2000 *Phys. Rev.* B **61** 10411
Goldoni A, Cepek C, Seta M D, Avila J, Asensio M C and Sancrotti M 2000 *Surf. Sci.* **454–456** 514
[35] Bertoni G, Cepek C and Sancrotti M 2003 *Appl. Surf. Sci.* **212/213** 52
[36] Rudolf P, Golden M S and Brühwiler P A 1999 *J. Electron Spectrosc. Relat. Phenom.* **100** 409
[37] Lof R W, Veenendaal M A V, Koopmans B, Jonkman H T and Sawatzky G A 1992 *Phys. Rev. Lett.* **68** 3924
[38] Brühwiler P A, Maxwell A J, Rudolf P, Gutleben C D, Wästberg B and Mårtensson N 1993 *Phys. Rev. Lett.* **71** 3721
[39] Brühwiler P A, Maxwell A J, Nilsson A, Mårtensson N and Gunnarsson O 1993 *Phys. Rev.* B **48** 18296
[40] For a review see Gunnarsson O 1997 *Rev. Mod. Phys.* **69** 575–606
[41] Hesper R, Tjeng L H and Sawatzky G A 1997 *Europhys. Lett.* **40** 177
[42] Bartynski R A, Jensen E, Gustafsson T and Plummer E W 1985 *Phys. Rev.* B **32** 1921
[43] Watson G M, Brühwiler P A, Plummer E W, Sagner H J and Frank K H 1990 *Phys. Rev. Lett.* **65** 468
[44] Tzeng C T, Yuh J Y, Lo W S, Chu R Y and Tsuei K D 2002 *J. Vac. Sci. Technol.* A **20** 1934
[45] Troullier N and Martins J L 1992 *Phys. Rev.* B **46** 1754
[46] Haddon R C, Brus L E and Raghavachari K 1986 *Chem. Phys. Lett.* **125** 459
[47] Pedio M, Grilli M L, Ottaviani C, Capozi M, Quaresima C, Perfetti P, Thiry P A, Caudano R and Rudolf P 1995 *J. Electron Spectrosc. Relat. Phenom.* **76** 405
[48] Rudolf P 1996 *Fullerenes and Fullerene Nanostructures* ed H Kuzmany, J Fink, M Mehring and S Roth (Singapore: World Scientific)
[49] Wertheim G K, Buchanan D N E, Chaban E E and Rowe J E 1992 *Solid State Commun.* **83** 785
[50] Rotenberg E, Enkvist C, Brühwiler P A, Maxwell A J and Mårtensson N 1996 *Phys. Rev.* B **54** R5279
[51] Hebard A F, Haddon R C, Fleming R M and Kortan A R 1991 *Appl. Phys. Lett.* **59** 2109
[52] Smith N V, Chen C T and Weinert M 1989 *Phys. Rev.* B **40** 7565
[53] Nilsson A, Björneholm O, Zdansky E O F, Tillborg H, Mårtensson N, Andersen J N and Nyholm R 1992 *Chem. Phys. Lett.* **197** 12
[54] Veenstra S C, Heeres A, Hadziioznnou G, Sawatzky G A and Jonkman H T 2002 *Appl. Phys.* A **75** 661
[55] Wang L L and Cheng H P 2004 *Phys. Rev.* B **69** 045404
[56] Ishii H, Sugiyama K, Ito E and Seki K 1999 *Adv. Mater.* **11** 605
[57] Koch N, Kahn A, Ghijsen J, Pireaux J J, Schwartz J, Johnson R L and Elschner A 2003 *Appl. Phys. Lett.* **82** 70
[58] Maxwell A J, Brühwiler P A, Arvanitis D, Hasselstrom J and Mårtensson N 1996 *Chem. Phys. Lett.* **260** 71
[59] Vries J D, Steger H, Kamke B, Menzel C, Weisser B, Kamke W and Hertel I V 1992 *Chem. Phys. Lett.* **188** 159
[60] Gensterblum G, Pireaux J J, Thiry P A, Caudano R, Vigneron J P, Lambin P, Lucas A A and Kratschmer W 1991 *Phys. Rev. Lett.* **67** 2171
[61] Wang X B, Ding C F and Wang L S 1999 *J. Chem. Phys.* **110** 8217
[62] Antropov V P, Gunnarsson O and Jepsen O 1992 *Phys. Rev.* B **46** R13647
[63] Pederson M R and Quong A A 1992 *Phys. Rev.* B **46** 13584